Improved Time-Frequency Representation of Multi-Component FM Signals with Compressed Observations

Vaishali S. Amin †, Yimin D. Zhang †, and Braham Himed ‡

† Department of Electrical and Computer Engineering, Temple University, Philadelphia, PA, 19122, USA
‡ RF Technology Branch, Air Force Research Laboratory, Dayton, OH, 45433, USA

***Abstract*—Compressed data measurements of non-stationary signals, which may arise from intentional signal undersampling or missing data samples, introduce undesirable artifacts in the rendered time-frequency (TF) representations. In particular, for multi-component non-linear frequency modulated (FM) signals with distinct amplitudes, such artifacts pose a great challenge to accurately reconstruct weaker signal components. In this paper, we develop improved TF representations that enable accurate instantaneous frequency estimation of such signals, achieve high energy concentration, and provide effective cross-term and artifact mitigation. The proposed technique utilizes a combination of iterative data interpolation in the time-lag domain to recover missing entries and a signal-adaptive TF kernel to suppress cross-terms and artifacts. Simulation results confirm the effectiveness of the proposed method.**

***Index Terms*—Frequency modulated signals, missing sample recovery, sparse reconstruction, time-frequency representation.**

I. Introduction

Time-frequency representation (TFR) is widely accepted as the most suitable technique for the representation, characterization, analysis and classification of frequency modulated (FM) signals, which are frequently observed in many radar, sonar, wireless communications, radio astronomy, audio, and biomedical applications [1]–[3]. For example, radar signal returns from maneuvering targets with different radar cross-sections are manifested as non-linear multi-component FM signals with a significant difference in their magnitude levels. In that case, the identification of weaker signal components poses a challenging scenario.

In practice, these signals are often received with compressed measurements that may arise from either missing samples or irregular sampling. In particular, missing observations may be the result of multipath fading, sensor failures, noise removal, and line-of-sight obstruction. However, irregular sampling schemes may be adopted due to sampling frequency limitations, logistical restrictions on data collections and storage, or simply to facilitate hardware simplification [4]–[7]. Depending upon the specific scenario, the missing samples can be either random or appear in groups. While the artifacts due to random missing samples uniformly spread in the entire time-frequency (TF) region, group missing samples render sinc-like artifact patterns clustered around true instantaneous frequencies (IFs) in TF regions, and thus hinder identification of true signal signatures, specifically the weaker ones [7].

The Wigner-Ville distribution (WVD), which is the simplest form of Cohen's class of quadratic TF distributions [8], exhibits severe cross-terms in the case of non-linear FM signals or multi-component FM signals. Signal-adaptive TF kernels are effective to mitigate the undesired effects of cross-terms and artifacts [9], [10]. However, the application of these TF kernels alone becomes insufficient when missing data appear in groups. Utilization of compressive sensing and sparse reconstruction techniques in conjunction with signal-adaptive TF kernels generally provides better TFR reconstruction results [7], [11]–[14]. However, these approaches may not provide effective auto-term identification of weaker signal components when non-linear FM signals have large variation in their amplitude levels, and in the presence of group missing samples. In such cases, the recently developed sparse reconstruction-based TF analysis techniques [15]–[18] perform relatively well in retrieving weaker signal components. However, these approaches either rely on the accuracy of the underlying TFRs, require cumbersome manual tuning of the parameters, are sensitive to frequency quantization errors, or suffer from high computational complexity.

The application of the missing data iterative adaptive approach (MIAA) [19] for missing data recovery in the instantaneous auto-correlation function (IAF) domain was first proposed in [20] for mono-component FM signals. This method was extended for reliable TFR recovery of multi-component FM signals in [7] by an iterative application of sparse reconstruction-based orthogonal matching pursuit (OMP) [21] in the IAF domain. However, when a non-linear FM signal has distinct amplitude levels and clustered missing samples, OMP-based approaches generally fail to provide an accurate reconstruction of the weaker signal components [15].

Motivated by these observations, in this paper, we propose a new non-parametric iterative approach that undertakes missing data recovery in the IAF domain through data interpolation using MIAA-based Capon spectrum estimation [22], [23], and in conjunction with a signal-adaptive TF kernel. Unlike the missing data iterative sparse reconstruction (MI-SR) method [7], in which a data-dependent TF kernel is used at the end

The work of V. S. Amin and Y. D. Zhang is supported in part by a contract with Matrix Research, Inc. for research sponsored by the Air Force Research Laboratory under Contract FA8650-14-D-1722. The work of Y. D. Zhang is also supported in part by a contract with Altamira Technologies Corp. for research sponsored by the Air Force Research Laboratory under Contract FA8650-18-C-1055.

of the iterative process, the proposed approach incorporates signal-adaptive TF kernels in the iterative process itself to improve TFR reconstruction performance. Compared to the iterative adaptive missing data recovery (IA-MDR) algorithm [24], the proposed approach exploiting an IAF averaging operation provides improved TFR reconstruction performance and is more suited for online implementation.

Using an appropriate combination of data interpolation in the IAF domain and signal-dependent TF kernel, the proposed approach provides improved TFRs of multi-component FM signals with an accurate high-resolution IF estimation, improved energy concentration and effective cross-terms/artifacts mitigation from compressed observations, in four important steps. The proposed technique works well for both random as well as group missing samples, and is particularly useful when the FM signal comprises multiple non-linear components with distinct amplitude levels, which demonstrate high proximity in the TF domain. The effectiveness of the proposed approach is verified through simulation results.

Notations. A lower (upper) case bold letter represents a vector (matrix). $(\cdot)^{\mathrm{T}}$, $(\cdot)^*$, and $(\cdot)^{\mathrm{H}}$, respectively, define transpose, complex conjugation, and conjugate transpose (Hermitian). $\mathcal{F}_x(\cdot)$ and $\mathcal{F}_x^{-1}(\cdot)$, respectively, define the discrete Fourier transform (DFT) and inverse DFT (IDFT) with respect to x. $\mathbf{I}_P$ represents a $P \times P$ identity matrix.

II. Quadratic TF Representations

A. Signal Model

Consider a K-component discrete-time FM signal, given by

$$s(t) = \sum_{k=1}^{K} s_k(t), \qquad t = 1, ..., T. \tag{1}$$

The kth signal component is expressed as

$$s_k(t) = a_k \exp(\jmath 2\pi \phi_k(t)), \qquad t = 1, ..., T, \tag{2}$$

where a_k $(a_1 \geq ... \geq a_K)$ and $\phi_k(t)$, respectively, denote the amplitude and time-varying phase of the kth signal component.

Let a $N \times T$ binary sampling matrix $\mathbf{\Lambda}$ maps the signal $\mathbf{s} = [s(1), ..., s(T)]^{\mathrm{T}}$, sampled using the Nyquist criterion, into the observed signal $\mathbf{r}$ consisting of a total number of N compressed observations that follow an irregular sampling scheme. Then, the observed signal $\mathbf{r}$ is represented as

$$\mathbf{r} = \mathbf{\Lambda s}. \tag{3}$$

We assume that a total number of $\bar{N} = T - N$ missing observations are clustered into B mutually non-overlapping groups, which are randomly distributed over time. The bth group contains $\bar{N}_b$ missing samples. Then, $\bar{N} = \sum_{b=1}^{B} \bar{N}_b$.

B. Joint Variable Domain Representations

The WVD of the observed signal is the one-dimensional (1-D) DFT of the respective IAF with respect to lag, τ, as

$$W_{rr}(t, f) = \mathcal{F}_\tau[C_{rr}(t, \tau)] = \sum_{\tau} C_{rr}(t, \tau) e^{-\jmath 4\pi f \tau}, \tag{4}$$

where the IAF of $r(t)$ is defined as

$$C_{rr}(t, \tau) = r\,(t + \tau)\, r^*\,(t - \tau)\,. \tag{5}$$

Similarly, the ambiguity function (AF) is obtained by taking the 1-D DFT of the respective IAF with respect to time, t, as

$$A_{rr}(\theta, \tau) = \mathcal{F}_t[C_{rr}(t, \tau)] = \sum_{t} C_{rr}(t, \tau) e^{-\jmath 2\pi \theta t}, \tag{6}$$

where θ is the frequency shift.

C. Signal-Adaptive TF Kernels

Signal-adaptive TF kernels [9], [10] effectively suppress cross-terms and missing data induced-artifacts. In this paper, we use the radially Gaussian kernel function-based adaptive optimal kernel (AOK) [9] as the signal-adaptive TF kernel, obtained as a solution to the following optimization problem:

$$\begin{aligned} \max_{\Phi} \int_0^{2\pi} \int_0^{\infty} & |A(\alpha, \psi)\Phi(\alpha, \psi)|^2 \alpha \, \mathrm{d}\alpha \, \mathrm{d}\psi \\ \text{subject to} \;\; & \Phi(\alpha, \psi) = \exp\Big(- \frac{\alpha^2}{2\sigma^2(\psi)} \Big), \\ & \frac{1}{4\pi^2} \int_0^{2\pi} \sigma^2(\psi) \, \mathrm{d}\psi \;\leq \beta, \end{aligned} \tag{7}$$

where $A(\alpha, \psi)$ is the time-localized, short-time ambiguity function defined in the polar coordinate, $\Phi(\alpha, \psi)$ is a Gaussian kernel function, $\psi = \arctan(\tau/\theta)$ is a radial angle, $\alpha = \sqrt{\theta^2 + \tau^2}$ is a radius, $\sigma(\psi)$ is the spread function that determines the spread of the Gaussian kernel at angle ψ, and parameter $\beta > 0$ controls the volume of the kernel.

After converting the kerneled AF in the polar coordinate system, $\breve{A}(\alpha, \psi) = A(\alpha, \psi)\Phi_{\mathrm{OPT}}(\alpha, \psi)$, to the rectangular coordinate system, $\breve{A}(\theta, \tau)$, the corresponding reduced-interference TFR can be obtained by taking the two-dimensional DFT of the kerneled AF, as

$$P_{\mathrm{AOK}}(t, f) = \mathcal{F}_\theta^{-1}\{\mathcal{F}_\tau[\breve{A}(\theta, \tau)]\}. \tag{8}$$

III. Proposed Method

In this section, we describe the proposed non-parametric iterative approach to achieve improved TFRs of multi-component FM signals that have distinct amplitude levels and contain compressed observations.

A. Problem Formulation

Let a K-sparse $Q \times 1$ TF vector $\mathbf{x}^{(t)}$ denote the column of underlying TFR $\mathbf{W}_{rr}$ at the tth time instant, where Q represents the total number of frequency grid points with f_q, $q = 1, ..., Q$, being the corresponding frequencies. As most of the elements of the vector $\mathbf{x}^{(t)}$ are zero or assume very small values, we usually have $K \ll Q$. In this paper, we choose the WVD (4) as the example of the underlying TFR. Let $\mathbf{D}$ define the $T \times Q$ 1-D IDFT matrix. Then, the corresponding $T \times 1$ IAF vector $\mathbf{y}^{(t)}$ is represented as

$$\mathbf{y}^{(t)} = \mathbf{D}\mathbf{x}^{(t)}, \quad t = 1, ..., T. \tag{9}$$

Most of the operations in this section are performed at each time instant t, unless otherwise specified. Hence, for notational simplicity, we omit superscript (t) from the subsequent expressions of $\mathbf{x}^{(t)}$ and $\mathbf{y}^{(t)}$.

Let P and $\bar{P} = T - P$, respectively, represent the total number of observed and missing IAF entries. Using the $P \times T$

masking matrix $\mathbf{\Psi}_r$ and the $\bar{P} \times T$ masking matrix $\mathbf{\Psi}_m$, we can extract the observed and missing entries of $\mathbf{y}$ into two components as

$$\mathbf{y}_r = \mathbf{\Psi}_r \mathbf{y}, \quad \mathbf{y}_m = \mathbf{\Psi}_m \mathbf{y}, \tag{10}$$

where vectors $\mathbf{y}_r = [y_{r_1}, y_{r_2}, ..., y_{r_P}]^{\mathrm{T}}$ and $\mathbf{y}_m = [y_{m_1}, y_{m_2}, ..., y_{m_{\bar{P}}}]^{\mathrm{T}}$, respectively, contain P measured and $\bar{P}$ missing IAF entries. Similarly, the rows of $\mathbf{D}$ corresponding to the elements of $\mathbf{y}_r$ and $\mathbf{y}_m$ are, respectively, extracted using the $P \times Q$ matrix $\mathbf{D}_r = \mathbf{\Psi}_r \mathbf{D}$ and the $\bar{P} \times Q$ matrix $\mathbf{D}_m = \mathbf{\Psi}_m \mathbf{D}$. Then, (9) can be related to the observed IAF entries as

$$\mathbf{y}_r = \mathbf{D}_r \mathbf{x}. \tag{11}$$

B. Proposed Technique

The proposed technique comprises the following four steps:

1) Iterative adaptive estimation of the spectral amplitudes from the available data and missing data recovery in the IAF domain for each time instant t;
2) Application of signal-adaptive TF kernel to obtain reduced interference TFR and associated IAF;
3) Averaging of the IAFs obtained at the end of the first two steps; and
4) Update of original missing IAF entries using the entries of the IAF obtained from the previous step.

In the following, we describe these key steps of the proposed method.

Initialization:

The outer iteration counter, i, is set to 1. The IAF vector of the observed entries, the corresponding IDFT matrix, and the corresponding data extraction matrix are, respectively, initialized as $\mathbf{y}_r^{[0]} = \mathbf{y}_r$, $\mathbf{D}_r^{[0]} = \mathbf{D}_r$, and $\mathbf{\Psi}_r^{[0]} = \mathbf{\Psi}_r$. Similarly, the IAF vector of the missing entries, the corresponding IDFT matrix, and the corresponding data extraction matrix are, respectively, initialized as $\mathbf{y}_m^{[0]} = \mathbf{y}_m$, $\mathbf{D}_m^{[0]} = \mathbf{D}_m$, and $\mathbf{\Psi}_m^{[0]} = \mathbf{\Psi}_m$. Note that the magnitudes of all the elements of $\mathbf{y}_m^{[0]}$ are almost zero (with the values smaller than 10^{-15}). The total number of available IAF entries is initialized as $P^{[0]} = P$, which represents the length of $\mathbf{y}_r^{[0]}$.

Iterative spectral amplitudes estimation and missing samples recovery:

The inner iteration counter, j, is set to 1. Let $x_q^{[i;j]}$ define the complex-valued spectral amplitude of $\mathbf{x}^{[i;j]}$ corresponding to frequency f_q at the $[i;j]$th iteration. The covariance matrix of the available IAF entries is initialized as $\mathbf{R}_r^{[i;j-1]} = \mathbf{I}_{P^{[i-1]}}$. The spectral amplitude corresponding to f_q is estimated as [22], [23],

$$\hat{x}_q^{[i;j]} = \frac{(\mathbf{d}_{rq}^{[i-1]})^{\mathrm{H}} (\mathbf{R}_r^{[i;j-1]})^{-1} \mathbf{y}_r^{[i-1]}}{(\mathbf{d}_{rq}^{[i-1]})^{\mathrm{H}} (\mathbf{R}_r^{[i;j-1]})^{-1} \mathbf{d}_{rq}^{[i-1]}}, \quad \forall q, \tag{12}$$

where $\mathbf{d}_{rq}^{[i-1]}$ represents the qth column of $\mathbf{D}_r^{[i-1]}$ corresponding to frequency f_q. Define $S_q^{[i;j]} = |\hat{x}_q^{[i;j]}|^2$. Then, the covariance matrix of the available IAF entries is updated as

$$\mathbf{R}_r^{[i;j]} = \sum_{q=1}^{Q} S_q^{[i;j]} \mathbf{d}_{rq}^{[i-1]} (\mathbf{d}_{rq}^{[i-1]})^{\mathrm{H}}. \tag{13}$$

The inner iteration counter, j, is incremented by one, and the values of $\hat{x}_q^{[i;j]}$ and $\mathbf{R}_r^{[i;j]}$ are iteratively updated until either the maximum number of iterations, j_{f}, is reached or $|\hat{x}_q^{[i;j]} - \hat{x}_q^{[i;j-1]}|$ is less than a predefined threshold ξ.

Based on $S_q^{[i;j_{\mathrm{f}}]}$ and the corresponding covariance matrix $\mathbf{R}_r^{[i;j_{\mathrm{f}}]}$, the missing IAF entries are recovered using the following minimum mean square error (MMSE) estimator [19],

$$\hat{\mathbf{y}}_m^{[i]} = \sum_{q=1}^{Q} S_q^{[i;j_{\mathrm{f}}]} (\mathbf{d}_{rq}^{[i-1]})^{\mathrm{H}} (\mathbf{R}_r^{[i;j_{\mathrm{f}}]})^{-1} \mathbf{y}_r^{[i-1]} \mathbf{d}_{mq}^{[i-1]}, \tag{14}$$

where $\mathbf{d}_{mq}^{[i-1]}$ is the qth column of $\mathbf{D}_m^{[i-1]}$ corresponding to frequency f_q. Then, the IAF vector $\hat{\mathbf{y}}_1^{[i]}$ is obtained as

$$\begin{aligned} \hat{\mathbf{y}}_1^{[i]} = {} & (\mathbf{\Psi}_m^{[i-1]})^{\mathrm{T}} (\mathbf{\Psi}_m^{[i-1]} (\mathbf{\Psi}_m^{[i-1]})^{\mathrm{T}})^{-1} \hat{\mathbf{y}}_m^{[i]} \\ & + (\mathbf{\Psi}_r^{[i-1]})^{\mathrm{T}} (\mathbf{\Psi}_r^{[i-1]} (\mathbf{\Psi}_r^{[i-1]})^{\mathrm{T}})^{-1} \mathbf{y}_r^{[i-1]}. \end{aligned} \tag{15}$$

The operations (12)–(15) are repeated for all time instants. Let $\hat{\mathbf{Y}}_1^{[i]}$ denote the $T \times T$ IAF matrix obtained by horizontally concatenating $\hat{\mathbf{y}}_1^{[i]}$ for all time instants.

Application of signal-adaptive TF kernel:

In the second stage, we apply the AOK [9] as the signal-adaptive TF kernel in order to mitigate the undesired effects of the cross-terms and artifacts from the respective TFR for further performance enhancement. Note that the AOK is optimized in the AF domain (7), where the AF is obtained from $\hat{\mathbf{Y}}_1^{[i]}$ based on the 1-D Fourier transform relationship (6) between them. The corresponding TFR is obtained using (8) for each time slice. Denote $\hat{\mathbf{x}}^{[i]}$ as the column of TFR obtained using AOK at the tth time instant. The corresponding IAF vector $\mathbf{y}_2^{[i]}$ is obtained by taking a 1-D IDFT of $\hat{\mathbf{x}}^{[i]}$ with respect to frequency f.

IAF averaging:

The interpolated IAF obtained after the first stage improves the estimation of auto-components in the respective TFR. However, TFR obtained using that result suffers from cross-terms and poor recovery performance of weaker signal components due to low energy of the interpolated IAF entries around the center values of the lag along the time axis. On the contrary, the IAF obtained from the AOK possesses high energy of IAF entries around the center values of τ along the time axis, which helps improve energy concentration and suppress cross-terms in the respective TFR.

In the third stage and based on the above observations, we average the IAFs obtained from the first two stages to combine the advantages offered by both, represented as

$$\hat{\mathbf{y}}_3^{[i]} = \frac{1}{2} \left(\hat{\mathbf{y}}_1^{[i]} + \hat{\mathbf{y}}_2^{[i]} \frac{\max |\hat{\mathbf{y}}_1^{[i]}|}{\max |\hat{\mathbf{y}}_2^{[i]}|} \right). \tag{16}$$

The IAF averaging operation in (16) provides superior TFR reconstruction results to [24], in which the interpolated IAF from the first stage is simply replaced by the IAF obtained using the signal-adaptive TF kernel. Note in (16) that the energy levels of the IAFs obtained after the first two stages are different. Therefore, in order to make the averaging effective, the energy levels of the second stage-IAF are mapped to the energy levels of the IAF obtained from the first stage in (16).

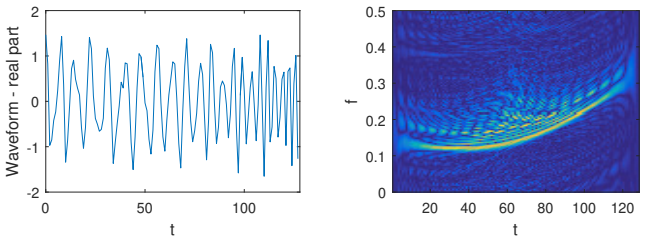

(a) (b)

Fig. 1 The original signal without missing samples (SNR 15 dB): (a) Real part; (b) WVD.

Update of original missing IAF entries:

We observe that, in order to ensure that missing data recovery and TF kernel do not introduce estimation bias in the subsequent iterations, it is important to retain the IAF entries associated with the observed signal. It is ensured by this fourth stage. The resulting updated IAF is obtained as

$$\hat{\mathbf{y}}^{[i]} = (\mathbf{\Psi}_m^{[0]})^{\mathrm{T}}(\mathbf{\Psi}_m^{[0]}(\mathbf{\Psi}_m^{[0]})^{\mathrm{T}})^{-1}\mathbf{\Psi}_m^{[0]}\hat{\mathbf{y}}_3^{[i]}\frac{\max|\mathbf{y}_r^{[0]}|}{\max|\hat{\mathbf{y}}_3^{[i]}|} + (\mathbf{\Psi}_r^{[0]})^{\mathrm{T}}(\mathbf{\Psi}_r^{[0]}(\mathbf{\Psi}_r^{[0]})^{\mathrm{T}})^{-1}\mathbf{y}_r^{[0]}. \quad (17)$$

Note in (17) that the energy levels of the IAF vector $\hat{\mathbf{y}}_3^{[i]}$ are mapped to the energy levels of the initial IAF $\mathbf{y}_r^{[0]}$. The entries of $\hat{\mathbf{y}}^{[i]}$ with amplitudes below a certain threshold ζ are marked as missing. The corresponding IAF vector of the missing entries, the IDFT matrix, and the data extraction matrix are, respectively, defined as $\mathbf{y}_m^{[i]}$, $\mathbf{D}_m^{[i]}$, and $\mathbf{\Psi}_m^{[i]}$. Similarly, the IAF vector of the observed entries, the corresponding IDFT matrix, data extraction matrix, and the total number of available IAF entries are, respectively, defined as $\mathbf{y}_r^{[i]}$, $\mathbf{D}_r^{[i]}$, $\mathbf{\Psi}_r^{[i]}$, and $P^{[i]}$.

The outer iteration counter, i, is incremented by one and the entire procedure is repeated until either the maximum number of iterations, i_{f}, is reached or the norm error between two subsequent signal estimates falls below a predefined threshold value, i.e.,

$$||\hat{\mathbf{x}}^{[i]} - \hat{\mathbf{x}}^{[i-1]}||_2^2 < \epsilon. \quad (18)$$

The final reduced interference TFR is obtained by horizontally concatenating $\hat{\mathbf{x}}^{[i_{\mathrm{f}}]}$ for all time instants, i.e.,

$$\mathbf{W}_{\mathrm{RID}} = [\hat{\mathbf{x}}_1^{[i_{\mathrm{f}}]}, ..., \hat{\mathbf{x}}_T^{[i_{\mathrm{f}}]}]. \quad (19)$$

IV. Simulation Results

To demonstrate the effectiveness of the proposed method, we consider a two-component non-linear FM signal with distinct amplitude levels of closely separated signatures in the TF domain, given by

$$s(t) = \exp(\jmath 2\pi\phi_1(t)) + 0.4\exp(\jmath 2\pi\phi_2(t)), \quad t = 1, ..., T, \quad (20)$$

where the phase laws of the two components are given by

$$\begin{aligned}\phi_1(t) &= 0.15t - 0.12t^2/T + 0.14t^3/T^2,\\ \phi_2(t) &= 0.25t - 0.15t^2/T + 0.15t^3/T^2.\end{aligned} \quad (21)$$

T and the signal-to-noise ratio (SNR) are, respectively, chosen to be 128 and 15 dB.

Fig. 1 shows the real part of the original signal waveform without missing samples and the corresponding WVD. As seen in Fig. 1(b), for this two-component non-linear FM signal, the WVD exhibits severe cross-terms between components, even without any missing samples. As a result, the weaker component cannot be clearly identified.

Fig. 2(a) shows the real part of the observed signal that contains a total of 48 (i.e., 37.5%) group missing samples, clustered into 12 groups that are randomly distributed over time. The number of missing samples in each group varies from 2 to 6. The position of missing samples are shown in red color in Fig. 2(a). The true IFs are provided in Fig. 2(h) for comparison purposes.

The group missing samples create convolutive sinc function-like patterns of artifacts that are concentrated near the true IFs in the TF region and misguide the identification of the true IFs. These patterns are clearly visible in the WVD depicted in Fig. 2(b). Figs. 2(c)–2(f), respectively, provide TFR reconstruction results obtained with the application of the MIAA in the IAF domain [20], the AOK [9], MISR applied to the kerneled IAF [7], and adaptive local filtering-based directional time-frequency distribution (ALF-DTFD) [15] to the observed signal. It is seen that, while all techniques are generally successful in retrieving the IFs of the stronger signal component, they either exhibit excessive cross-terms and artifacts that hinder identification of true signal signatures (e.g., MIAA in Fig. 2(c)) or provide erroneous results of the weaker signal component, specifically, when these components share high proximity in the TF domain. As clearly seen in Fig. 2(d), signal-adaptive TF kernel (e.g., AOK in this case) alone cannot mitigate all artifacts due to burst missing samples.

As evident from Fig. 2(g), the proposed method provides superior TFR reconstruction results with high resolution of the estimated signal components and improved energy concentration of the underlying TFR. The proposed method effectively suppresses cross-terms and artifacts from the TFR and, at the same time, preserves the auto-term TF distributions. The achieved TFR benefits from the suitable combination of data interpolation in the IAF domain and the cross-term suppression capabilities of signal-adaptive TF kernel. For the considered scenario, three iterations of the proposed method are applied with the AOK volume is chosen as 3.

Usually, 2 to 5 iterations of the proposed method are sufficient to reconstruct the desired high-resolution TFR. The significant improvement in terms of auto-component reconstruction and cross-terms/artifacts mitigation is observed within the initial 2 to 3 iterations, as most of the missing entries are updated by this time. Beyond that, each additional iteration provides less significant improvements in terms of energy enhancement and IF estimation accuracy.

V. Conclusions

In this paper, we proposed a new non-parametric iterative approach that effectively combines missing samples recovery in the IAF domain and an application of signal-adaptive TF kernel to achieve improved TFRs of multi-component FM signals with compressed observations. The proposed method

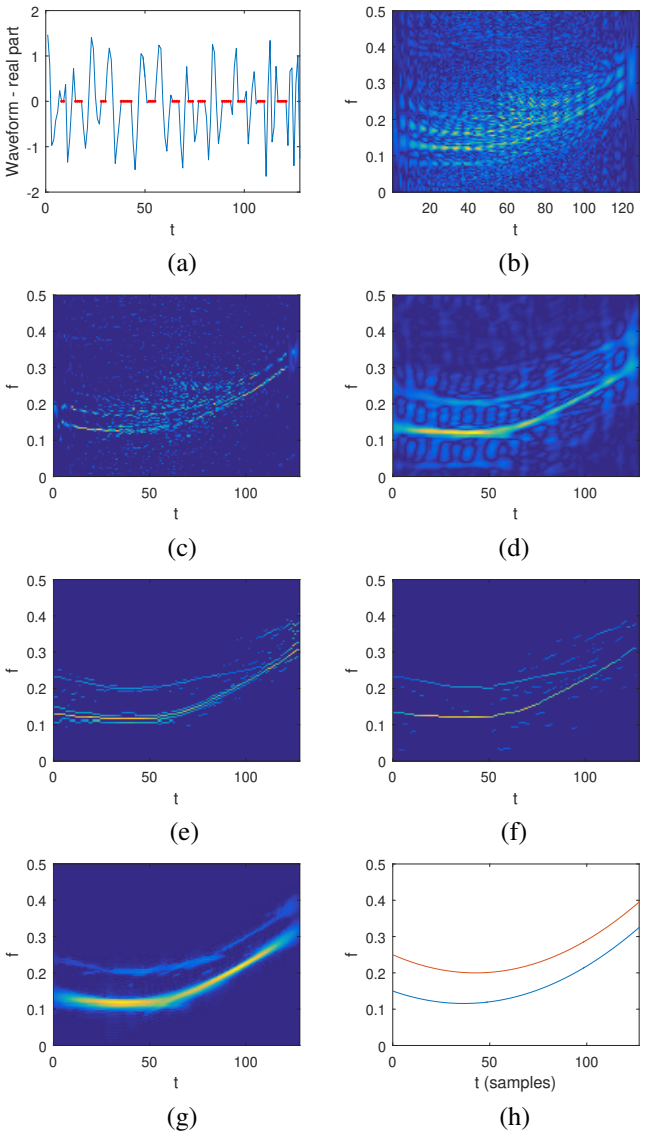

Fig. 2 TFRs obtained using different methods on the observed signal with 37.5% group missing samples (SNR 15dB): (a) Real part of the observed signal (with missing data positions marked in red color); (b) WVD; (c) MIAA applied to IAF; (d) AOK (volume 3); (e) MI-SR applied to the kerneled IAF; (f) ALF-DTFD; (g) Proposed method; (h) True IFs (for comparison).

provides accurate high-resolution estimation of signal auto-term signatures and effective cross-term/artifact mitigation. In particular, the proposed approach is effective in reconstructing the TFR of the weaker signal components when multi-component signals contain group missing samples and have non-linear, closely separated signatures with distinct amplitude levels. Simulation results confirmed the superiority of the proposed technique over state-of-the-art techniques.

REFERENCES

[1] B. Boashash, "Estimating and interpreting the instantaneous frequency of a signal – Part 2: Algorithms and applications," *Proc. IEEE*, vol. 80, no. 4, pp. 540–568, Apr. 1992.

[2] L. Cohen, *Time-Frequency Analysis: Theory and Applications*. Prentice-Hall, 1995.

[3] V. Chen and H. Ling, *Time-Frequency Transforms for Radar Imaging and Signal Analysis*. Artech House, 2002.

[4] F. Marvasti (Ed.), *Nonuniform Sampling: Theory and Practice*. Springer Science and Business Media, 2001.

[5] E. Larsson and J. Li, "Spectral analysis of periodically gapped data," *IEEE Trans. Aerosp. Electron. Syst.*, vol. 39, no. 3, pp. 1089–1097, July 2003.

[6] Y. Wang, J. Li, and P. Stoica, *Spectral Analysis of Signals: The Missing Data Case*. Morgan and Claypool Publishers, 2006.

[7] V. S. Amin, Y. D. Zhang, and B. Himed, "Sparsity-based time-frequency representation of FM signals with burst missing samples," *Signal Process.*, vol. 155, pp. 25–43, Feb. 2019.

[8] L. Cohen, "Time-frequency distributions – A review," *Proc. IEEE*, vol. 77, no. 7, pp. 941–981, July 1989.

[9] D. L. Jones and R. G. Baraniuk, "An adaptive optimal-kernel time-frequency representation," *IEEE Trans. Signal Process.*, vol. 43, no. 10, pp. 2361–2371, Oct. 1995.

[10] N. Khan and B. Boashash, "Multi-component instantaneous frequency estimation using locally adaptive directional time frequency distributions," *Int. J. Adaptive Control Signal Process.*, vol. 30, pp. 429–442, Mar. 2016.

[11] Q. Wu, Y. D. Zhang, and M. G. Amin, "Continuous structure based Bayesian compressive sensing for sparse reconstruction of time-frequency distributions," in *Proc. Int. Conf. Digital Signal Process.*, Hong Kong, China, Aug. 2014, pp. 831–836.

[12] L. Stankovic, S. Stankovic, I. Orovic, and Y. D. Zhang, "Time-frequency analysis of micro-Doppler signals based on compressive sensing," in M. Amin (ed.), *Compressive Sensing for Urban Radars*, CRC Press, 2014.

[13] B. Jokanovic and M. G. Amin, "Reduced interference sparse time-frequency distributions for compressed observations," *IEEE Trans. Signal Process.*, vol. 63, no. 24, pp. 6698–6709, Dec. 2015.

[14] M. G. Amin, B. Jokanovic, Y. D. Zhang, and F. Ahmad, "A sparsity-perspective to quadratic time-frequency distributions," *Digital Signal Process.*, vol. 46, pp. 175–190, Nov. 2015.

[15] V. S. Amin, Y. D. Zhang, and B. Himed, "Improved instantaneous frequency estimation of multi-component FM signals," in *Proc. IEEE Radar Conf.*, Boston, MA, Apr. 2019, pp. 1–6.

[16] V. S. Amin, Y. D. Zhang, and B. Himed, "Sequential time-frequency signature estimation of multi-component FM signals," in *Proc. IEEE Asilomar Conf. Signals Syst. Comp.*, Pacific Grove, CA, Nov. 2019, pp. 1901–1905.

[17] S. Zhang and Y. D. Zhang, "Robust time-frequency analysis of multiple FM signals with burst missing samples," *IEEE Signal Process. Lett.*, vol. 26, no. 8, pp. 1172–1176, June 2019.

[18] S. Zhang and Y. D. Zhang, "Low-rank Hankel matrix completion for robust time-frequency analysis," *IEEE Trans. Signal Process.*, vol. 68, pp. 6171–6186, Oct. 2020.

[19] P. Stoica, J. Li, and J. Ling, "Missing data recovery via a non-parametric iterative adaptive approach," *IEEE Signal Process. Lett.*, vol. 16, no. 4, pp. 241–244, Apr. 2009.

[20] Y. D. Zhang, "Resilient quadratic time-frequency distribution for FM signals with gapped missing data," in *Proc. IEEE Radar Conf.*, Seattle, WA, May 2017, pp. 1765–1769.

[21] J. A. Tropp and A. C. Gilbert, "Signal recovery from random measurements via orthogonal matching pursuit," *IEEE Trans. Inf. Theory*, vol. 53, no. 12, pp. 4655–4666, Dec. 2007.

[22] P. Stoica and R. L. Moses, *Spectral Analysis of Signals*. Prentice-Hall, 2005.

[23] T. Yardibi, J. Li, P. Stoica, M. Xue, and A. B. Baggeroer, "Source localization and sensing: A nonparametric iterative adaptive approach based on weighted least squares," *IEEE Trans. Aerosp. Electron. Syst.*, vol. 46, no. 1, pp. 425–443, Jan. 2010.

[24] V. S. Amin, Y. D. Zhang, and B. Himed, "Improved IF estimation of multi-component FM signals through iterative adaptive missing data recovery," in *Proc. IEEE Radar Conf.*, Florence, Italy, Sept. 2020.